

Time–temperature profiles of multi-layer actuators

J. Pritchard, R. Ramesh, C.R. Bowen*

Department of Engineering and Applied Science, Materials Research Centre, University of Bath, Bath BA2 7AY, UK

Received 5 November 2003; received in revised form 8 April 2004; accepted 16 April 2004

Available online 4 June 2004

Abstract

During accelerated testing of actuators, relatively high frequencies and electric fields are used and the resulting heat generation and self-heating of the actuator due to ferroelectric hysteresis loss becomes of increasing concern. It is therefore important to have knowledge of parameters such as the predicted actuator temperature, total loss per cycle and the overall heat transfer coefficient of the system. The heat generation in multi-layer actuators is studied as a function of driving frequency and applied electric field. The heat transfer coefficients and the total hysteresis loss per cycle in the device are estimated from fitting experimental data to analytical expressions of time–temperature profiles. The temperature rise is found to be approximately proportional to the frequency, while the total loss of the actuator per cycle increases with applied field and frequency. The high estimated values of heat transfer coefficient, which range from 140 to 210 W m⁻² K⁻¹, are due to the high conductivity and thermal mass of the sample holder.

© 2004 Elsevier B.V. All rights reserved.

Keywords: Piezoelectric; Multi-layer; Actuator; Loss mechanism

1. Introduction

Multi-layer actuator (MLA) devices are of interest as their thin piezoelectric layers (<100 μm) enable the production of large electric fields, and high strain, at relatively low operating voltages. The low voltage, high displacement characteristics of MLAs enable them to be used in a variety of applications such as semiconductor manufacturing, fuel injection systems, ink-jet printer heads, camera auto focus and shutter devices [1–3]. In order to maximise the piezoelectric displacement, soft lead zirconate titanate (PZT) materials are often used [4,5]. These materials have high piezoelectric strain coefficients (such as d_{33} and d_{31}), but as a consequence also have high losses that can lead to significant self-heating of the actuator at its operating conditions [6]. Härdtl stated that ferroelectric losses originate from four main mechanisms, namely domain wall motion, a fundamental lattice loss, a microstructural loss and a conductivity loss [7]. At high electric fields (>1 kV mm⁻¹) and at low frequencies, where domains can follow the applied electric field ferroelectric, hysteresis due to domain wall motion is the main contributor to the loss process [7–9].

1.1. Temperature increase

Zheng et al. developed a useful method to study the heat generation in piezoelectric actuators under stress-free conditions [8]. The temperature rise of an actuator can be estimated by the expression:

$$\Delta T = \frac{ufv_e}{k(T)A} \quad (1)$$

where ΔT is the temperature rise (K); u the total dielectric loss of the actuator per unit volume per driving cycle (J mm⁻³) and in this case is primarily due to hysteresis; f the driving frequency (Hz); v_e the active volume of the actuator (m³); A the total surface area of the actuator (m²); and $k(T)$ the overall heat transfer coefficient (W m⁻² K⁻¹).

Eq. (1) states that the temperature rise increases with increasing drive frequency, total hysteresis loss per cycle and amount of active material (for a specific surface area). As hysteresis losses increase with electric field due to domain wall motion and an associated increase in the area of the polarisation–field hysteresis loop, the temperature rise of the actuator increases with applied electric field. Eq. (1) also indicates that the use of a large surface area actuator or a high heat transfer coefficient environment (e.g. by placing the actuator in an oil bath) can reduce the temperature increase.

* Corresponding author. Tel.: +44-1225-323660;
fax: +44-1225-386098.
E-mail address: msscrb@bath.ac.uk (C.R. Bowen).

Table 1
Dimensions and material constants of multi-layer actuators

Dimensions of actuator	10 mm × 10 mm × 3 mm
Surface area of actuator (<i>A</i>)	320 mm ²
No. of layers	29
Thickness of individual layers	90 μm
Active volume (<i>v_e</i>)	8 mm × 8 mm × 2.8 mm
Density of PZT (<i>ρ</i>)	7500 kg m ⁻³ [14]
Specific heat capacity of PZT (<i>c</i>)	420 J kg ⁻¹ K ⁻¹ [15]
Thermal conductivity steatite (<i>k_s</i>)	2–2.5 W m ⁻¹ K ⁻¹ (manufacturers data)

1.2. Time–temperature profile

While Eq. (1) describes the steady state temperature rise of an actuator, the time–temperature profile of the actuator can be expressed in the form [8]:

$$T = T_0 + \Delta T(1 - e^{-t/\tau}) \quad (2)$$

where *t* is the instantaneous time (s); *τ* the time constant (s⁻¹); *T*₀ the initial actuator temperature (K); *T* the actuator temperature at time *t* (K); and *ΔT* the maximum temperature rise of the actuator (K). From Eq. (2), at *t* = 0, then *T* = *T*₀ and at equilibrium when *t* → ∞, *T* = *T*₀ + *ΔT*, as would be expected. The time constant (*τ*) in Eq. (1) is defined by

$$\tau = \frac{v\rho c}{k(T)A} \quad (3)$$

where *v* is the total actuator volume (m³); *ρ* the density of the actuator (kg m⁻³); and *c* the specific heat capacity of actuator (J kg⁻¹ K⁻¹). In this work the density and specific heat capacity of the bulk PZT material (Table 1) has been used and the influence of the electrode material (a silver–palladium alloy) has been neglected since the volume fraction of electrode material in the actuator is small (<10%).

2. Aims

In the present work, we have studied the effect of electric field and frequency on heat generation in multi-layer actuators. The actuators were placed within an accelerated measurement system to evaluate the fatigue and time dependent properties of the actuators as a function of number of cycles, applied electric field and mechanical stress. Fig. 1 shows an image of the experimental set-up, where a number of rectangular actuators are placed in an insulating steatite sample holder that is 10 mm thick and attached to a large steel base plate. A cover plate (not shown in Fig. 1) is placed in contact with the top surface of the actuators and is used to apply a mechanical stress during testing, which also consists of a 10 mm electrically insulating steatite section attached to a large steel plate.

During accelerated testing, relatively high frequencies (up to 1 kHz) are used so that the testing period for a specific number of ac cycles (10⁸ to 10⁹) is not excessively long [10].

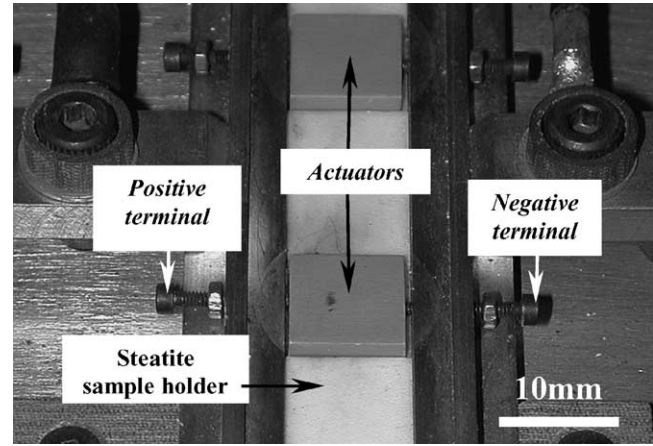


Fig. 1. Actuator location in measurement system, without cover plate.

In addition to high frequencies, high electric fields (up to 3 kV mm⁻¹) are used and heat generation due to increased hysteresis (*P–E* loss) becomes of increasing concern as it can lead to premature and unrepresentative degradation of actuator performance by depolarisation, domain pinning, enhanced migration of electrode ions (such as silver) or oxygen vacancies under a unipolar ac voltage [11–13]. Therefore, it is important to have knowledge of parameters such as the predicted actuator temperature, total loss per cycle and the total heat transfer coefficient of the system.

The heat transfer characteristics strongly depend on the experimental set-up. Actuators that are freely suspended in air display relatively low heat transfer coefficients, between 20 and 40 W m⁻² K⁻¹ since convection and radiation is the primary heat transfer mechanism [8]. During testing of the rectangular actuators used in this study, whose dimensions are in Table 1, each face of the actuator is in contact with the sample holder and therefore a much higher overall heat transfer coefficient is expected, primarily due to thermal conduction from the actuator into the sample holder. The heat transfer of the system can be expressed as

energy generated within actuator

$$- \text{energy conducted into sample holder} \\ = \text{change in internal energy of actuator} \quad (4)$$

The energy generated per second with the actuator is effectively *uv_ef* [8]. The overall heat transfer coefficient, which includes conduction, convection and radiation, is *k(T)*. Therefore Eq. (4) becomes [8]:

$$ufv_e - k(T)A(T - T_0) = v\rho c \frac{dT}{dt} \quad (5)$$

As the steel base plate and cover plate have a relatively high thermal conductivity (~45 W m⁻¹ K⁻¹) and its mass is large compared to the actuator and steatite component, it is assumed that steatite surfaces in contact with the steel maintain an ambient temperature. The energy conducted through into sample holder per second is therefore given by *k_sA(T – T₀)/Δx* where *Δx* is the thickness of the steatite

sample holder (10 mm), k_s is the thermal conductivity of steatite ($\text{W m}^{-1} \text{K}^{-1}$), T is the temperature of the actuator (K) and T_0 is the temperature as the steatite–steel interface (ambient). Eq. (5) therefore becomes

$$ufv_e - \frac{k_s A (T - T_0)}{\Delta x} = \nu \rho c \frac{dT}{dt} \quad (6)$$

The solution of Eq. (6) effectively yields Eqs. (1) and (3), where in this case the heat transfer coefficient $k(T)$ in Eqs. (1), (3) and (5) is $k_s/\Delta x$. Using the thermal conductivity of steatite in Table 1 and $\Delta x = 10$ mm, the expected value of $k(T)$ is 200–250 $\text{W m}^{-2} \text{K}^{-1}$. Since there is a limited change in k_s with temperature up to 100 °C, $k(T)$ is expected to be approximately constant in the temperature range studied.

3. Predicted temperature profiles

Fig. 2 shows predicted time–temperature profiles of the actuators studied, where Eq. (1) is used to calculate the rise in temperature (ΔT) and Eq. (2) is used to calculate the time–temperature response. The data is calculated based on the ρ , c , A , v , and v_e values in Table 1, with an operating frequency of 500 Hz and a typical total loss per cycle of 5 kJ m^{-3} . A variety of heat transfer coefficients have been used, ranging from 20 $\text{W m}^{-2} \text{K}^{-1}$ (typical for free air convection [8]) to 200 $\text{W m}^{-2} \text{K}^{-1}$ (the value calculated in Section 2). Fig. 2 shows that as the heat transfer coefficient is decreased there is an increase in the temperature rise and a longer time is required for the temperature of the actuator to reach a plateau and steady state conditions.

4. Experimental

The temperature profiles of actuators were monitored using a thermocouple data acquisition system with no mechanical stress applied. Three samples were freely placed on the

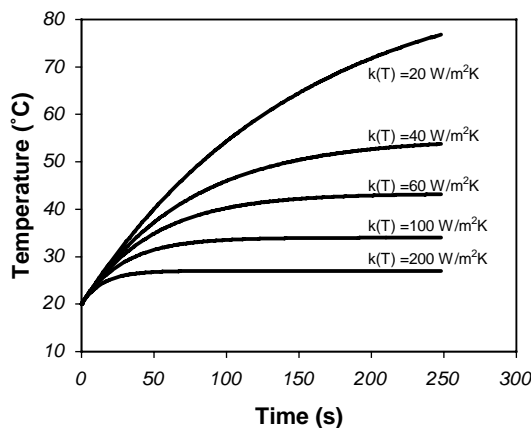


Fig. 2. Time–temperature profiles for a variety of heat transfer coefficients using Eqs. (1) and (2). The frequency is 500 Hz, total loss per cycle is 5 kJ m^{-3} and the materials and geometrical constants in Table 1.

steatite sample holders and a thermocouple was attached to the surface of each sample. The actuators were electrically driven by a variety of sinusoidal ac voltages (frequencies and peak to peak magnitudes), onto which a dc bias was superimposed in order to have a unipolar operation and maintain the polarity of the actuators tested. Once the unipolar voltage was applied, the instantaneous temperature of the sample was recorded at an interval of 2 s for a total time of 1000 s, a time sufficient for the actuator to reach steady state conditions based on the results in Fig. 2. Temperature profiles for various test conditions (0–100, 0–150, 0–200, 0–250 V peak to peak at 50, 100, 500 Hz and 1 kHz) were collected. Three samples were tested at each experimental condition and the average data were taken for the analysis. Full details of the dimensions and material constants of the devices are given in Table 1.

5. Results

Fig. 3a shows the temperature profiles recorded at 50 Hz and various driving voltages, namely 100, 150, 200 and 250 V which corresponds to maximum electric fields of 1.1, 1.7, 2.2 and 2.8 kV mm^{-1} , respectively, given that the thickness of the layers and the inter-electrode distance of the actuators were 90 μm .

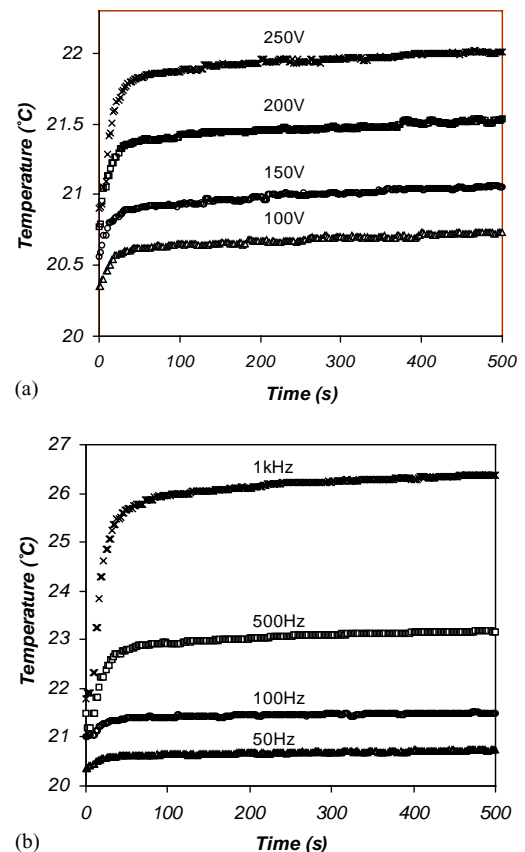


Fig. 3. Time–temperature profile of multi-layer actuators at: (a) 50 Hz and various drive voltages; (b) 100 V peak-to-peak at various frequencies.

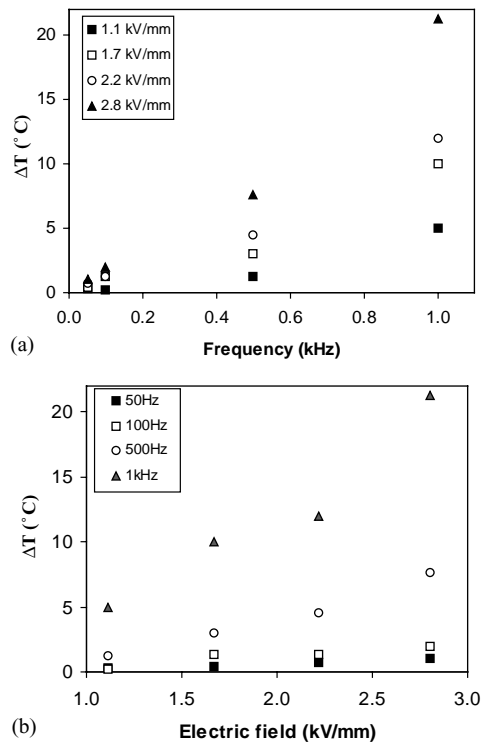


Fig. 4. (a) Temperature rise vs. frequency at different applied voltages; (b) temperature rise vs. applied electric field at different frequencies.

Similar trends were observed for all the frequency conditions tested and only the results at 50 Hz is plotted in the figure for the purpose of clarity. At time $t = 0$, the driving voltage is applied and the temperature of the actuator rapidly increases and reaches a plateau. The rapid time to reach a plateau (<200 s) and low plateau temperature suggest a relatively high heat transfer coefficient, on comparing Fig. 3a with predicted curves in Fig. 2 for various $k(T)$ values. Fig. 3b shows similar time–temperature data for a constant applied electric field (1.1 kV mm^{-1}) at various frequencies.

The observed temperature increases are summarised in Fig. 4. The temperature rise versus frequency is shown in Fig. 4a for different applied electric fields. The temperature rise (ΔT) increases approximately linearly with frequency, as expected from Eq. (1), although it should be indicated that the total loss per cycle, u , and heat transfer coefficient, $k(T)$ may also be a function of frequency and temperature [8,16]. It is observed that the temperature increase of the device is also dependent on the applied electric field, as shown in Fig. 4b. This is primarily due to the increase in total polarisation–field (P – E) hysteresis loss per cycle [7,9,16].

A typical representative time–temperature profile of an actuator is shown in Fig. 5, for the test condition 1 kHz and 150 V ac. The experimental data points are fitted to Eq. (2), which allows the estimation of the time constant (τ) with close agreement between the experimental data and fitted curve from Eq. (2). The experimental data fits well with the model during the initial period of testing, but deviates slightly for longer times ($t > 100$ s) in that the temperature

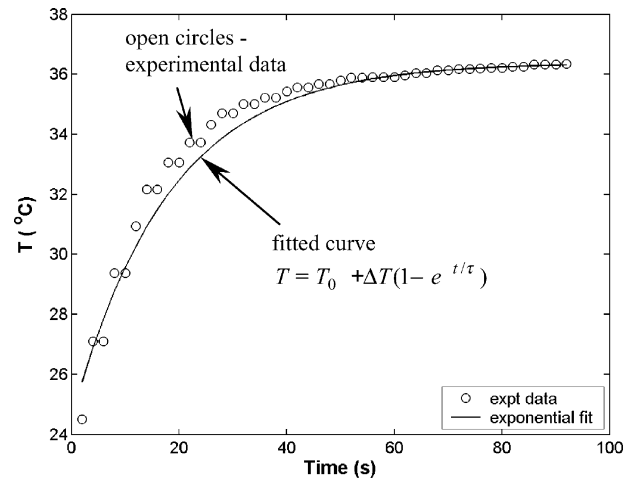


Fig. 5. Comparison of model and experimental data of instantaneous temperature with time at 1 kHz and 150 V ac.

should attain an equilibrium and a steady state temperature, as in Fig. 2. Fig. 3 shows that after reaching a plateau after 100 s there is a small gradual increase in temperature with time, unlike freely suspended samples where equilibrium is more readily attained. This is probably due to the fact that the sample holder is large in comparison to the actuator dimensions and there is gradual heating of the sample holder and steel base by the actuator and pure equilibrium is not attained. Therefore, only data from the first 100 s of testing are considered for the present analysis.

The values of τ are calculated from fitting the time–temperature data are used to calculate the overall heat transfer coefficients $k(T)$ using Eq. (3), knowing the values of v , ρ , c and A in Table 1. Fig. 6a and b shows calculated $k(T)$ values as a function of frequency and applied electric field, respectively. The increase in heat transfer coefficient with electric field for freely suspended actuators has been attributed to increased convection due to increased vibration of the actuator at higher fields [8]. In this case the increase in $k(T)$ with increasing field (Fig. 6a) may also be due to an increase in convection along small air gaps between the actuator and sample holder or due to the increased strain and improved contact between the actuator and sample holder. The estimated values of $k(T)$ range from 140 to $210 \text{ W m}^{-2} \text{ K}^{-1}$ which is in agreement with the predicted value of 200 – $250 \text{ W m}^{-2} \text{ K}^{-1}$ since the estimation neglects contact thermal resistance. These values are significantly higher than those calculated by Zheng et al. (20 – $40 \text{ W m}^{-2} \text{ K}^{-1}$) for actuators suspended in air. These high values of heat transfer coefficients are attributed to the heat being dissipated through the sample holder which is in direct contact with the top and bottom faces ($10 \text{ mm} \times 10 \text{ mm}$) of the actuator. This is particularly advantageous for a variety of practical applications and accelerated testing as it minimises self-heating of the actuators driven by a high electric field. For the case of actuators suspended in air, the rise in temperature (ΔT) can be in excess of 140 °C,

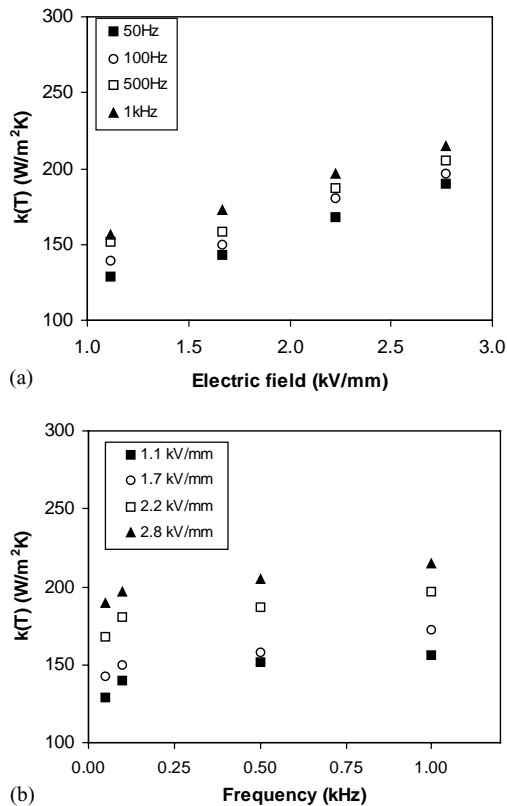


Fig. 6. (a) Effect of electric field on $k(T)$ values of MLA devices; (b) effect of frequency field on $k(T)$ values.

whereas, it is less than 25 °C in the present case. Higher heat transfer coefficient values would be expected by decreasing the steatite thickness (Δx) in Eq. (6).

Once $k(T)$ has been calculated for particular conditions of field and frequency, the total loss per driving cycle per unit volume (u) of the actuators can be determined using Eq. (1) and the measured values of ΔT and $k(T)$. Since u is calculated directly from the temperature response it includes all the possible loss mechanism contributing to heat generation. The variation in total loss as a function of applied electric field for different frequencies are shown in Fig. 7. The loss is found to increase with applied electric field (E) and, as stated, is primarily due to the ferroelectric hysteresis loss, although the mechanical losses may become significant when the actuator is driven at a frequency close to resonance [16]. No clear relationship is observed between loss and frequency, since hysteresis loss does not vary significantly within the frequency range studied [9,16]. In the present study, the frequency of the applied voltage is below 1 kHz, whereas the resonance frequency of the device is 140 kHz. Therefore, it is reasonable to assume that the mechanical losses are negligible and the hysteresis loss is considered to be the major contributor to the total loss. The values of u , which have been determined under unipolar operation, are relatively small ($< 10 \text{ kJ m}^{-3}$) in comparison to those under bipolar operation where full polarisation reversal occurs at high fields [17].

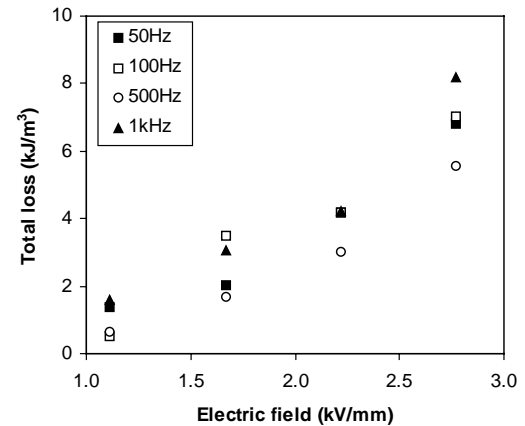


Fig. 7. Effect of applied electric field on total loss per cycle per unit volume (u) at different frequencies.

6. Conclusions

The heat generation in multi-layer actuators was analysed at various frequencies and applied electric fields. The heat transfer coefficients and the total loss in the device were estimated by fitting experimental data to analytical expressions of the time–temperature profiles. High values of the heat transfer coefficients obtained in the present study were attributed to the high thermal mass of the sample holder with agreement with measured and estimated heat transfer coefficients. The high $k(T)$ facilitates rapid dissipation of heat generated in the multi-layer actuators, ensuring relatively small temperature increases and rapid attainment of near steady state conditions.

The equations are useful tools in assessing the heat generation and temperature rise of actuators as a function of operating conditions (frequency, electric field magnitude and polarity, actuator mounting, etc.) and materials properties (hysteresis loss). This is important in accelerated lifetime testing of these devices where the frequency or electric field are often increased to reduce testing time, which can lead to overheating of the actuator and thermal degradation, depolarisation or enhanced migration of electrode materials (such as Ag) by diffusion. It can also be used for estimation of device operating temperature since this will influence other piezoelectric properties such as piezoelectric coefficients (such as d_{33} and d_{31}) and permittivity (device capacitance). Extrapolation of data outside the regime experimentally examined (stress, frequency and electric field) should be undertaken with care due to additional loss mechanisms contributing to heat generation.

Acknowledgements

The authors would like to acknowledge Qinetiq. One of the authors (RR) is grateful to the Department of Science and Technology, New Delhi, India, for the financial assistance under BOYSCAST scheme.

References

- [1] K. Uchino, Ceramic actuators: principles and applications, *Mater. Res. Soc. Bull.* 18 (1993) 42–47.
- [2] K. Uchino, S. Takahashi, in: M.W. Roberos, J. White (Eds.), *Multilayer Ceramic Actuators*, *Curr. Opin. Solid State Mater. Sci.* 1 (1996) 698–705.
- [3] C. Schuh, Th. Steinkopff, A. Wolff, K. Lubitz, Piezoceramic multilayer actuators for fuel injection systems in automotive area, *Smart Structures and Materials 2000: Active Materials*, *Proc. SPIE* 3992 (2000) 165–175.
- [4] T.A. Wheat, A. Ahmad, R.K. Minhas, Ceramic actuators: materials, *J. Can. Ceram. Soc.* 69 (1999) 56–61.
- [5] J.W.C. de Vries, Functional behaviour of multilayer actuators with inactive parts, *Sens. Actuators A* 72 (1999) 251–255.
- [6] A. Ochi, S. Takahashi, S. Tagami, Temperature characteristics for multilayer piezoelectric ceramic actuator, *J. Appl. Phys.* 24 (Suppl. 3) (1985) 209–212.
- [7] K.H. Härdtl, Electrical and mechanical losses in ferroelectric ceramics, *Ceram. Int.* 8 (1982) 121–128.
- [8] J. Zheng, S. Takahashi, S. Yoshikawa, K. Uchino, J.W.C. de Vries, Heat generation in multilayer piezoelectric actuators, *J. Am. Ceram. Soc.* 79 (1996) 3193.
- [9] H.J. Hagemann, Loss mechanisms and domain stabilisation in BaTiO₃, *J. Phys. C: Solid State Phys.* 11 (1978) 3333–3344.
- [10] U. Kumar, M. Randall, J. Hock, A. Ritter, Reliability studies on electrostrictive actuators, *J. Int. Mater. Sys. Struct.* 5 (1994) 802–808.
- [11] K. Nagata, S. Kinoshita, Relationship between lifetime and multilayer ceramic actuator temperature, *Jpn. J. Appl. Phys.* 32 (1995) 5266–5269.
- [12] J. Thomgrueng, T. Tsuchiya, K. Nagata, Lifetime and degradation mechanisms of multilayer ceramic actuator, *Jpn. J. Appl. Phys.* 37 (1998) 5306–5310.
- [13] M.H. Lente, J.A.L. Eiras, Interrelationship between self-heating and ferroelectric properties in PZT ceramics during polarization reorientation, *J. Phys.-Condens. Matter* 12 (2000) 5939–5950.
- [14] H.A. Kunkel, S. Locke, B. Pikeroen, Finite-element analysis of vibrational modes in piezoelectric ceramic disks, *IEEE Trans. Ultrason. Ferroelectr. Freq. Contr.* 37 (1990) 316–328.
- [15] N. Abboud, J. Mould, G. Wojcik, D. Vaughan, D. Powell, V. Murray, C. MacLean, Thermal generation, diffusion and dissipation in 1–3 piezocomposite sonar transducers: finite element analysis and experimental measurements, in: S.C. Schneider, M. Levy, B.R. McAvoy (Eds.), *Proceedings of the IEEE Ultrasonics Symposium*, vols. 1 and 2, 1997, pp. 895–900.
- [16] K. Uchino, S. Hirose, Loss mechanisms in piezoelectrics: how to measure different losses separately, *IEEE Trans. Ultrason. Ferroelectr. Freq. Contr.* 48 (2001) 307–321.
- [17] P.M. Chaplya, G.P. Carman, Dielectric and piezoelectric response of lead zirconate–lead titanate at high electric and mechanical loads in terms of non-180 degrees domain wall motion, *J. Appl. Phys.* 90 (2001) 5278–5286.

Biographies

J. Pritchard graduated in 1995 from the Department of Materials Science and Engineering, University of Bath and received her PhD in ‘Fatigue and creep performance of wood products in standard and high humidity environments’ in 1999 at the same University. After her PhD she conducted postdoctoral research on multilayer actuators and is now at the UK Centre for Materials Education, University of Liverpool.

R. Ramesh received his masters degree in Physics, MPhil and PhD in 1987 from Barathiar University, Coimbatore, in 1989 from Anna University, Madras and in 1994 from Indian Institute of Technology, Madras, India, respectively. He worked as a post doctoral fellow in IIT, Madras and a visiting scientist in IGCAR, Kalpakkam, India for 1 year each. Since 1996, he has been working as a researcher in NPOL, Cochin. He was awarded BOYSCAST research fellowship and has been working as a visiting fellow at the Department of Engineering and Applied Science, University of Bath, UK. His areas of specialisation include piezoelectric transducers, analytical and numerical modelling of acoustic devices.

C.R. Bowen graduated with a degree in Materials Science from the University of Bath in 1990 and received his DPhil in processing of ceramic composites in 1994 from the Department of Materials, University of Oxford. He is now a Lecturer at the Department of Engineering and Applied Science, University of Bath. His current research includes processing and characterisation of structural and functional ceramic materials.